ACTA CHEMICA SCANDINAVICA 24 (1970) 1036–1050

Heat Capacities and Thermodynamic Properties of the $Ni_{1-x}Se$-Phase from 298 to 1050°K

FREDRIK GRØNVOLD

Kjemisk Institutt A, Universitetet i Oslo, Blindern, Oslo 3, Norway

Heat capacities of nickel selenides with compositions $Ni_{19}Se_{20}$, Ni_7Se_8 and Ni_4Se_5 have been measured in the range 298 to 1050°K by adiabatic shield calorimetry with intermittent heating and temperature equilibration between inputs. The samples represent the $Ni_{1-x}Se$-phase with NiAs-like structures and a varying number of metal vacancies. $Ni_{19}Se_{20}$ is without transitions and shows a regularly increasing heat capacity up to 1050°K. The entropy and enthalpy increments ($X°_{1000} - X°_{298}$) are 34.83 J °K^{-1} and 20.64 kJ for 1/39 mole $Ni_{19}Se_{20}$. For Ni_7Se_8 a λ-type transition occurs with maximum heat capacity at 503°K. The associated entropy increment is 0.96 J °K^{-1} for 1/15 mole Ni_7Se_8 and related to the disorder of vacancies within every other nickel layer parallel to 001. The entropy and enthalpy increments between 298 and 1000°K, including those of the transition, are 35.83 J °K^{-1} and 21.25 kJ for 1/15 mole Ni_7Se_8. For Ni_4Se_5 two λ-type transitions are observed with maxima at 589 and 995°K and entropy increments of 0.47 and 0.13 J °K^{-1} per 1/9 mole Ni_4Se_5, respectively. Both transitions are probably related to the disorder of vacancies within every other metal layer. The entropy and enthalpy increments between 298 and 1000°K, including those of the transitions, are 35.65 J °K^{-1} and 21.30 kJ for 1/9 mole Ni_4Se_5.

The $Ni_{1-x}Se$-phase with NiAs-like structures has been shown[1] to exist in the composition range $Ni_{0.98}Se$ to $Ni_{0.77}Se$ for samples heat-treated at 400 and 550°C. Two superstructures were noted, an orthorhombic one with $A = a\sqrt{3}$, $B = 3a$, and $C = 3c$ at the composition $Ni_{0.87}Se$, and a monoclinic one below $Ni_{0.83}Se$, with $A = a\sqrt{3}$, $B = a$, and $C = 2c$ and $\beta = 90.52°$ at the composition $Ni_{0.80}Se$. The vacancy distribution and atomic parameters for a sample with the latter composition have been ascertained.[2] Curiously enough, and in contrast to the results by Hiller and Wegener,[3] neither the 1:1 nor the 3:4 stoichiometric ratios between nickel and selenium were found to be within the homogeneity range of this phase, and further studies were obviously needed. Some high-temperature enthalpy of formation data for the $Ni_{1-x}Se$-phase have been reported,[4] and also low temperature heat capacities in the range 5 to 350°K for three samples within the homogeneity range of the phase.[5]

In the latter study normal sigmate behavior was observed, except for slightly augmenting heat capacity values for the two samples richer in selenium above 250°K. Transitions might therefore be expected in these samples at higher temperatures.

In the present study heat capacities of samples with the same compositions, *i.e.* $Ni_{19}Se_{20}$ (or $Ni_{0.95}Se$), Ni_7Se_8 (or $Ni_{0.875}Se$) and Ni_4Se_5 (or $Ni_{0.80}Se$) have been measured in the range 298 to 1050°K in order to ascertain the presence of any transitions in the compounds and to provide necessary data for a thermodynamic characterization of the non-stoichiometric $Ni_{1-x}Se$-phase. Some high temperature X-ray powder photographs of the samples have also been taken.

EXPERIMENTAL

A. Samples. The nickel selenides were made by fusion of high purity nickel and selenium in evacuated and sealed quartz tubes for 2 h at 1000°C. They were then cooled to room temperature in the furnace, crushed and transferred to new tubes. After annealing at 550°C for 7 days the samples were cooled to room temperature over a period of 2 days.

The nickel used was prepared from "Nickel oxide, low in cobalt and iron" from the British Drug Houses, Ltd. by reduction with hydrogen gas first at 500°C for 5 h and then at 1000°C for 2 h. Spectrographic analyses showed the presence of the following impurities (in ppm): Al(100), Ba(1), Ca(10), Co(10), Cr(1), Cu(1), Fe(10), Mg(50), Mn(1), and Si(50).

The high-purity selenium was a gift from Bolidens Gruvaktiebolag. It was reported to contain these impurities (in ppm): Cl(2), Fe(0.8), K(0.3), Na(0.4), and non-volatile matter (12). The following elements were not detected (the numbers indicate the sensitivity limit in ppm): Ag(0.03), Al(0.3), As(1), Bi(0.1), Ca(1), Cr(0.3), Cu(0.1), Hg(0.5), Mg(0.3), Mn(0.1), Ni(0.3), Pb(0.3), S(5), Si(1), Sn(0.3), Te(1) and Zn(1).

The weighed-in compositions of the three samples were $Ni_{19}Se_{20}$, Ni_7Se_8 and Ni_4Se_5, taking the atomic weights of nickel and selenium to be 58.71 and 78.96, respectively.

After the heat treatment the major part of the samples was transferred to the quartz ampoules for heat capacity measurements. The mass of samples used was 161.767 g $Ni_{19}Se_{20}$, 175.907 g Ni_7Se_8, and 151.428 g Ni_4Se_5.

B. Calorimeter. Measurements were made in a previously described calorimeter[1] operated with adiabatic shields and intermittent energy inputs and temperature equilibration between each input. The 50 cm^3 sample containers have a well for the heater and platinum resistance thermometer, axially located in the cylindrical silver calorimeter. The calorimeter-sample assembly is located inside a double-walled shield system with enclosed heaters. Outside the shields is a heated guard system of silver. The whole assembly is placed in a vertical tube furnace.

The temperature differences between corresponding parts of calorimeter and shields are measured by means of Pt/Pt 10 % Rh thermopiles. The amplified signals are recorded and also used for automatic control of the energy input to the shield heaters to maintain quasi-adiabatic conditions during input and drift periods. The temperature of the guard body is kept automatically 0.4°C below that of the shield, while the temperature of the furnace windings is kept 10°C lower to secure satisfactory operation of the control units.

Heat capacity measurements of the empty calorimeter assembly were carried out in separate series of experiments. They represented from 43 to 46 % of the total heat capacity outside the transition region in case of the old calorimeter (Mark III) and from 50 to 56 % in case of the new one (Mark IV).

Small corrections were applied for the differences in mass of the quartz containers, for temperature excursions of the shields from the calorimeter temperature, and for "zero" drift of the calorimeter.

The thermometer resistance was measured with a Mueller bridge (Leeds & Northrup Model 8072 for the later measurements), and the derived temperatures were judged to correspond with the International Practical Temperature Scale (1948) to within 0.1°C.

Table 1. Heat capacities of nickel selenides, joule mole^{-1} °K^{-1}.

1/39 $Ni_{19}Se_{20}$
(1 mole $Ni_{0.487}$ $Se_{0.513}$ ≙ 69.09 g)

T, °K	C_p
Series I	
313.68	25.89
329.49	26.08
344.94	26.24
360.03	26.47
370.71	26.75
377.14	26.44
387.58	26.75
401.91	26.90
416.03	26.96
Series II	
423.55	26.92
437.21	27.24
450.66	27.33
463.97	27.47
477.15	27.63
Series III	
481.80	27.47
494.76	27.71
507.58	27.77
520.28	27.99
532.91	27.97
545.45	28.02
557.89	28.37
570.26	28.46
582.57	28.43
594.81	28.61
606.97	28.74
Series IV	
707.45	29.95
719.64	30.34
731.80	30.48
743.91	30.61
755.98	30.73
768.01	30.75
779.99	30.88
791.93	31.03
803.82	31.30
815.69	31.42
827.48	31.64
Series V	
819.12	31.29
832.54	31.65
845.89	31.85
859.17	32.08
872.40	32.06
885.56	32.21
898.64	32.51
911.66	32.80
924.61	32.98
Series VI	
918.65	32.81
932.32	32.95
945.90	33.03
959.38	33.56
972.79	33.75
986.11	34.14
999.36	34.38
1012.54	34.58
1026.61	35.26
1038.59	35.68
1051.48	36.20
New calorimeter (IV)	
Series VII	
715.61	29.91
727.28	30.04
739.67	30.22
752.02	30.29
764.32	30.53
776.56	30.66
788.74	30.99
800.88	30.79
Series VIII	
590.44	28.73
602.65	28.81
616.40	29.02
630.05	29.12
643.63	29.20
657.13	29.37
670.57	29.47
690.00	29.58

1/15 Ni_7Se_8
(1 mole $Ni_{0.467}$ $Se_{0.533}$ ≙ 69.51 g)

T, °K	C_p
Series I	
300.35	25.64
313.36	25.95
326.22	26.21
338.89	26.30
351.39	26.59
363.71	26.79
375.88	26.99
Series II	
623.33	29.54
634.78	29.37
646.15	29.49
657.45	29.60
668.69	29.67
679.86	29.95
691.08	29.61
Series III	
691.31	30.20
702.92	30.29
714.50	30.33
734.18	30.43
745.68	30.77
757.14	30.71
768.59	30.84
780.00	31.03
791.39	31.02
802.74	31.13
814.05	31.28
825.29	31.42
Series IV	
811.43	31.34
822.60	31.48
860.23	31.96
873.05	32.37
885.81	32.39
898.48	32.71
911.11	32.75
923.65	32.98
936.15	33.25
Series V	
914.36	32.87
927.45	32.92
940.43	33.19
953.36	33.44

Table 1. Continued.

966.20	33.71
978.97	33.84
991.70	34.07
1004.38	34.32

New calorimeter (IV)

Series VI

411.64	27.59
424.33	27.94
436.86	28.27
449.24	28.60
461.48	29.42
485.48	30.51
493.99	36.77
499.13	41.35
503.23	43.73
507.65	32.20
513.36	29.98
519.19	29.49
525.06	29.65
530.92	29.34

Series VII

537.79	29.22
550.34	29.08
563.80	29.13
577.21	29.03
590.56	29.14
603.84	29.22
617.05	29.34
630.19	29.41
643.25	29.52
656.26	29.62
669.19	29.77
682.06	29.82
694.88	29.89
707.63	30.07

Series VIII

304.65	25.71
318.85	26.02
332.72	26.30
346.15	26.49
359.39	26.74
372.47	26.92
385.45	27.09
398.18	27.35
410.76	27.58
423.21	27.86
435.51	28.21
447.65	28.64
459.65	29.08

Series IX

472.41	29.74
482.93	30.66
488.56	31.41
492.68	34.93
495.23	40.40
497.66	41.17
499.54	42.48
500.85	43.14
502.15	44.58
503.43	45.36
504.70	44.96
506.69	33.21
509.43	30.76
512.61	30.64
516.40	30.48
521.98	30.39
527.55	30.40
533.13	29.68
538.76	29.21
544.39	29.19

Series X

502.56	44.96
507.37	33.27
512.66	30.79
518.03	30.62
523.40	30.54
528.75	30.49
534.14	29.70
539.57	29.48
544.99	29.32
550.41	29.31

Series XI

505.17	38.40
515.51	30.56
523.61	30.56
529.00	30.51
534.40	29.67

1/9 Ni_4Se_5
(1 mole $Ni_{0.444}$ $Se_{0.556}$ ≙ 69.96 g)

Series I

T, °K	C_p
589.37	33.69
603.45	29.72
617.85	29.74
632.18	29.91
646.42	29.97
660.56	30.18
674.62	30.43
688.60	30.47
702.51	30.60
716.35	30.66

Series II

722.44	30.92
736.92	30.92
751.28	31.03
765.58	31.17
779.84	31.34
794.07	31.56
808.25	31.58
822.35	31.77
836.37	32.05
850.31	32.43
864.17	32.49
877.95	32.89
891.65	33.02

Series III

904.85	33.34
918.27	33.63
931.60	34.00
944.84	34.30
957.98	34.73
971.03	35.02
984.00	35.63
996.94	35.10
1009.93	34.54
1022.90	34.68
1035.81	35.03

Series IV

546.60	30.01
557.62	31.59
568.36	32.72
578.88	34.01
589.21	34.66
599.80	30.02
610.69	29.92
621.57	29.95
632.41	29.94
643.19	29.98

Series V

962.16	35.01
971.59	35.33
980.99	35.40

Table 1. Continued.

990.30	35.77
997.29	36.17
1002.00	34.45
1006.70	34.66
1013.72	34.94
1024.57	35.13
1036.89	35.63
1048.40	35.32

New calorimeter (IV)

Series VI

343.80	26.25
355.90	26.41
367.87	26.50
379.70	26.64
391.41	26.80
402.98	26.94
414.45	27.04
425.81	27.15
437.06	27.28

Series VII

447.24	27.48
458.24	27.60
470.05	27.76
482.66	27.90
495.19	28.05
507.56	28.36
520.66	28.82
534.47	29.34

Series VIII

526.84	29.36
532.78	29.55
537.21	29.56
540.15	29.86
543.08	29.90
546.01	30.07
548.92	30.33
551.81	30.86
554.67	31.64
557.51	32.10
560.33	32.16
563.14	32.42
565.94	32.63
568.73	33.04
571.47	33.09
574.20	33.38

Series IX

551.32	30.88
554.23	30.95
555.65	31.43
557.10	31.53
558.55	31.68
559.96	32.02
561.40	31.88
562.84	31.91
564.23	32.23
565.63	32.11
567.02	32.27

Series X

557.96	32.22
559.18	32.21
560.13	32.47
561.08	32.52
562.03	31.98
562.98	32.46
563.93	32.65
569.46	33.03
581.11	34.52
588.93	35.77
591.38	34.36
593.89	31.41
596.47	30.08
599.06	29.99
602.98	29.89
608.19	30.00
615.94	30.08

Precision is considerably better and the temperature increments are probably accurate to 0.01°C after corrections for quasi-adiabatic drift. The energy inputs were measured with a double microvolt potentiometer (Rubicon Model 2773), a calibrated standard cell and a gating counter (Beckman Model 7416) operated by a quartz crystal oscillator. The accuracy of the energy inputs is better than 0.02 %.

C. X-Ray data. Lattice constant data were obtained in a 19 cm diameter Unicam high temperature camera with copper radiation [$\lambda(\mathrm{Cu}K\alpha_1) = 1.54051$ Å]. The samples were sealed in thin-walled quartz capillaries. By means of a voltage regulator the temperature was kept constant within ± 3°C during an exposure. The Pt/PtRh thermocouples of the furnace were calibrated with a standard couple located at the position of the specimen, and the temperatures given probably represent the sample temperature within ± 5°C. The estimated standard deviation in the lattice constant values is less than 0.05 %.

RESULTS

The heat-capacity determinations of the three nickel selenides are listed in Table 1 in chronological order. They are given for 1 mole of mixture Ni_xSe_{1-x} at the mean temperature of the energy input. The approximate temperature increments can usually be inferred from the adjacent mean temperature values.

For $Ni_{19}Se_{20}$ the heat capacity values increase almost linearly with temperature up to 900°K, see Fig. 1. Above this temperature a steadily increasing temperature dependence is observed up to 1050°K, the limiting temperature

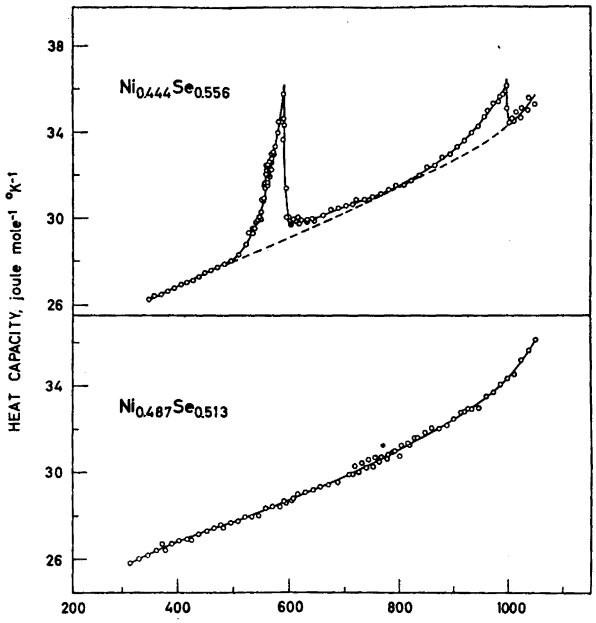

Fig. 1. Heat capacities of 1/39 mole $Ni_{19}Se_{20}$ and 1/9 mole Ni_4Se_5 as functions of temperature. -- represents estimated non-cooperative heat capacity in transition regions for Ni_4Se_5.

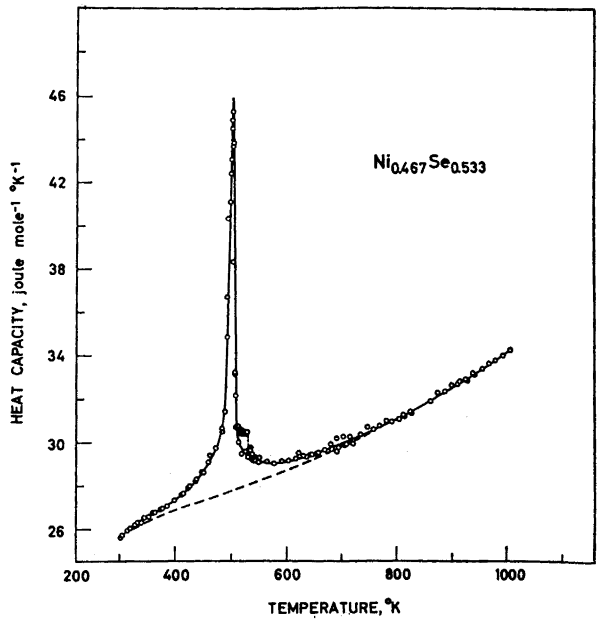

Fig. 2. Heat capacity of 1/15 mole Ni_7Se_8 as function of temperature. -- represents estimated non-cooperative heat capacity in the transition region.

Table 2. Thermodynamic properties of nickel selenides, joule mole^{-1} °K^{-1}.

	1/39 $Ni_{19}Se_{20}$			1/15 Ni_7Se_8			1/9 Ni_4Se_5		
T, °K	(1 mole $Ni_{0.487}$ $Se_{0.513}$ ≙ 69.09 g)			(1 mole $Ni_{0.467}$ $Se_{0.533}$ ≙ 69.51 g)			(1 mole $Ni_{0.444}$ $Se_{0.556}$ ≙ 69.96 g)		
	C_p	$S°-S_0°$	$\frac{H°-H_0°}{T}$	C_p	$S°-S_0°$	$\frac{H°-H_0°}{T}$	C_p	$S°-S_0°$	$\frac{H°-H_0°}{T}$
298.15	25.75	36.627	17.908	25.63	36.016	17.667	25.27	35.589	17.500
300	25.77	36.786	17.956	25.67	36.175	17.716	25.29	35.744	17.548
320	26.01	38.461	18.452	26.08	37.850	18.227	25.67	37.392	18.043
340	26.23	40.049	18.903	26.42	39.440	18.699	26.05	38.958	18.503
360	26.46	41.554	19.317	26.73	40.958	19.137	26.39	40.456	18.932
380	26.66	42.991	19.698	27.03	42.413	19.544	26.66	41.889	19.332
400	26.87	44.365	20.052	27.39	43.810	19.928	26.89	43.264	19.705
420	27.06	45.681	20.381	27.79	45.157	20.292	27.10	44.582	20.052
440	27.24	46.944	20.689	28.34	46.462	20.645	27.33	45.848	20.378
460	27.43	48.159	20.987	29.09	47.736	20.994	27.59	47.068	20.685
480	27.62	49.325	21.250	30.28	48.990	21.353	27.87	48.243	20.979
500	27.80	50.461	21.509	42.43	50.397	21.874	28.22	49.392	21.261
520	27.98	51.553	21.754	29.63	51.751	22.356	28.75	50.506	21.538
540	28.17	52.614	21.988	29.20	52.861	22.617	29.67	51.613	21.821
560	28.36	53.642	22.212	29.07	53.920	22.849	32.36	52.732	22.139
580	28.56	54.638	22.428	29.10	54.938	23.064	34.26	53.889	22.512
600	28.76	55.615	22.636	29.20	55.931	23.267	30.02	55.011	22.864
620	28.96	56.558	22.836	29.34	56.888	23.460	29.83	55.990	23.089
640	29.17	57.481	23.031	29.51	57.823	23.647	29.99	56.939	23.302
660	29.38	58.378	23.220	29.70	58.730	23.827	30.16	57.864	23.508
680	29.61	59.261	23.405	29.90	59.622	24.003	30.34	58.770	23.706
700	29.86	60.124	23.586	30.10	60.492	24.177	30.54	59.653	23.898
720	30.11	60.966	23.763	30.30	61.340	24.345	30.73	60.513	24.085
740	30.37	61.794	23.938	30.51	62.173	24.508	30.92	61.358	24.267
760	30.64	62.609	24.111	30.74	62.991	24.669	31.12	62.186	24.445
780	30.90	63.410	24.282	30.96	63.793	24.828	31.32	62.998	24.619
800	31.17	64.196	24.451	31.20	64.580	24.984	31.56	63.794	24.789
820	31.43	64.967	24.618	31.44	65.351	25.139	31.84	64.575	24.958
840	31.69	65.730	24.783	31.71	66.114	25.292	32.14	65.348	25.125
860	31.95	66.477	24.947	32.00	66.862	25.445	32.46	66.107	25.292
880	32.22	67.217	25.109	32.29	67.602	25.597	32.82	66.859	25.459
900	32.51	67.940	25.270	32.59	68.326	25.749	33.24	67.597	25.627
920	32.82	68.662	25.431	32.90	69.050	25.901	33.68	68.337	25.797
940	33.14	69.368	25.592	33.22	69.758	26.053	34.22	69.064	25.971
960	33.49	70.074	25.753	33.55	70.465	26.206	34.81	69.795	26.148
980	33.90	70.765	25.915	33.88	71.156	26.359	35.47	70.516	26.332
1000	34.40	71.457	26.079	34.23	71.846	26.513	34.88	71.239	26.519
1020	35.01	72.144	26.248	(34.58) [a]	(72.527)	(26.668)	34.62	71.928	26.682
1040	35.72	72.828	26.424	(34.93)	(73.199)	(26.823)	35.19	72.608	26.844
1050	36.11	73.175	26.529	(35.13)	(73.538)	(26.902)	35.58	72.952	26.927

[a] Extrapolated values.

of the experiments. This increase is probably caused by disproportionation of the sample.

In case of Ni_7Se_8 a regular λ-type transition connected with the disorder of vacancies is observed with maximum at 503°K, see Fig. 2. No further transitions are observed except for a small anomaly around 530°K. It was not observed in the earlier measurements, but only after the sample had been transferred to a new container and reheated to above 1000°K (Series X and XI). The anomaly is presumably caused by the presence of a small amount of nickel monoxide. In this compound a heat capacity maximum occurs at 525°K due to the antiferro- to paramagnetic transition, and the presence of about 1 mole % NiO explains the enhanced heat capacity of the selenide in this region.

In Ni_4Se_5 two λ-type transitions are observed, one with maximum at 589°K, the other with maximum around 995°K, see Fig. 1. They are both probably related to changes in the vacancy ordering. The 589°K transition has a rather unusual shape, as if it contained a smaller maximum around 560°K. Two additional series of experiments (IX and X) also indicate a maximum in this region.

Values of the thermodynamic properties for the three samples have been calculated using graphically interpolated values from the smoothly drawn heat capacity curves. The entropy and enthalpy increments were computed by numerical integration. For $Ni_{19}Se_{20}$ the heat capacity data were also represented by a least squares fitted polynomial expression. The two sets of data agree to within 0.15 % for the heat capacity and to within 0.05 % for the derived functions. Values of $S°-S_0°$ and $(H°-H_0°)/T$ are listed in Table 2 for every 20°K after incorporation of the previously [5] determined values of $S_{298}°-S_0°$ and $(H_{298}°-H_0°)/T$.

The estimated standard deviation of the individual heat capacity values from the smooth curve is 0.39 % for $Ni_{19}Se_{20}$. It is 0.42 % for Ni_7Se_8 and 0.52 % for Ni_4Se_5 after exclusion of eight and four measurements, respectively, which deviated more than 2 % from the curve. The values of entropy and enthalpy are considered to be accurate to ± 0.3 %, but additional digits are given in the tables because of their importance on a relative scale. Gibbs energy values are not given because of uncertainty as to the presence of complete structural order in the samples below 5°K.

DISCUSSION AND SUPPLEMENTARY X-RAY DATA

A. $Ni_{19}Se_{20}$. The results for $Ni_{19}Se_{20}$ differ from those of the other two samples in that no λ-type transition is observed. Apparently, the vacancy concentration is insufficient for ordering to take place in $Ni_{19}Se_{20}$, which probably means that the ordering temperature lies below the temperature at which metal atom or vacancy diffusion ceases. It is still uncertain whether the vacancies are distributed at random over all metal positions or not. If they only occur in every other metal layer perpendicular to the *c*-axis, the structure might be considered as a transition link between NiAs and the $Cd(OH)_2$ structure types. So far it has definitely been established that Ni_4Se_5, which contains 20 % metal vacancies, represents such a transition link, and

the same is probably true for Ni_7Se_8. Accordingly, $Ni_{19}Se_{20}$ is expected to have zero-point entropy of the order

$$\Delta S_0^\circ = -(R/2)(0.9 \ln 0.9 + 0.1 \ln 0.1)$$
$$= 1.35 \text{ J °K}^{-1} \text{ per mole } Ni_{0.95}Se.$$

X-Ray powder photographs of $Ni_{19}Se_{20}$ taken at several temperatures up to about 500°C confirm presence of the hexagonal structure only, with lattice constants and unit cell volume as given in Table 3 and Fig. 3. The volume

Table 3. Lattice constants and cell volume for $Ni_{19}Se_{20}$. Units: °C, Å.

T	a	c	V
20	3.652	5.347	61.76
110	3.657	5.363	62.12
200	3.661	5.379	62.44
305	3.666	5.403	62.89
415	3.668	5.418	63.13
490	3.670	5.429	63.33

expansion coefficient, β, is of normal magnitude, but decreases from about 7×10^{-5} to 3.5×10^{-5} °C^{-1} in this range.

Disregarding now any other contributions ot the heat capacity at constant volume, the heat capacity at constant pressure can be calculated as outlined

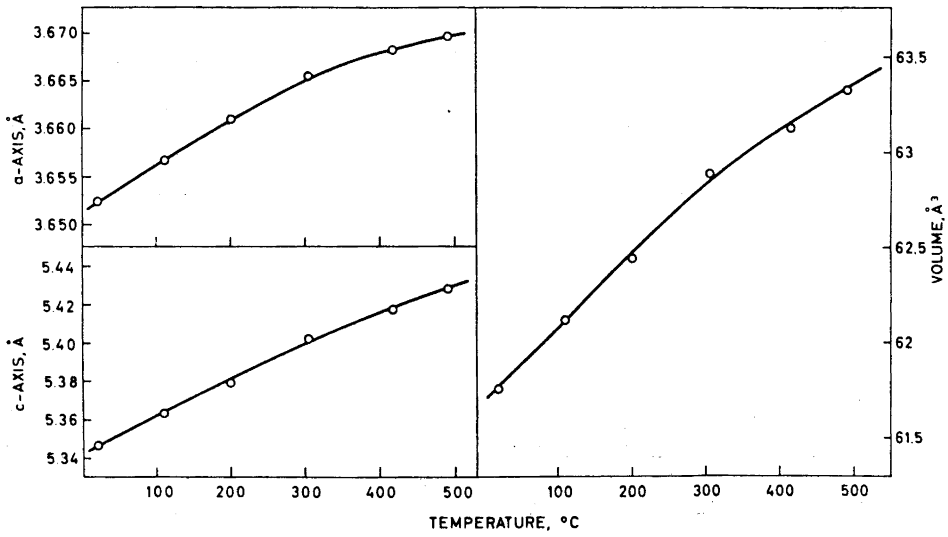

Fig. 3. Lattice constants and cell volume for $Ni_{19}Se_{20}$.

for the iron selenides.[7] Results are shown in Fig. 4 for a single Debye function with $\theta = 270°K$ and a dilation contribution according to Nernst and Lindemann:[8]

$$C_d = C_p - C_v = A\,(T/T_f)\,C_p^2$$

where $A = 0.0051$ mole °K J^{-1} and T_f is the melting temperature of the substance ($T_f \approx 1200°K$ according to Kuznetsov *et al.*[9]).

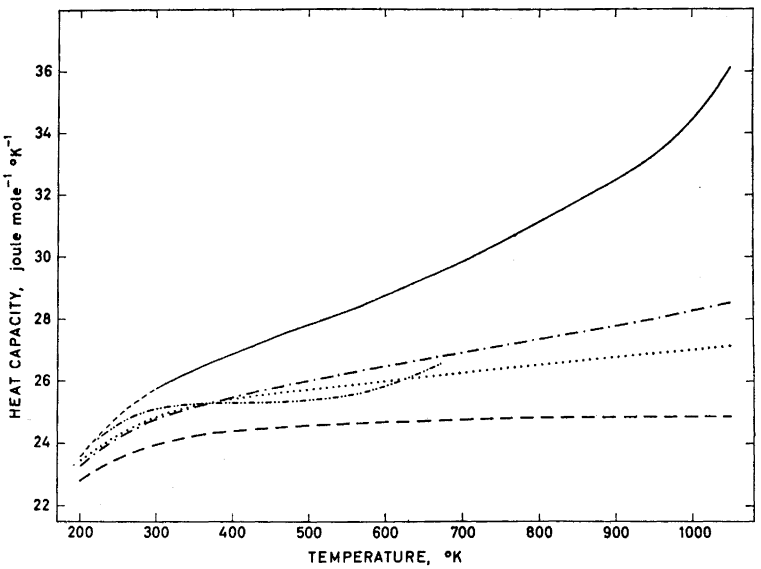

Fig. 4. Attempted resolution of the heat capacity of $Ni_{19}Se_{20}$. ——— represents observed data, ------ represents C_v in the harmonic approximation, —·— represents C_v plus Nernst-Lindemann dilation contribution, ····· represents C_v plus Grüneisen dilation contribution, —··— represents experimental data minus Schottky contribution assuming $g_1/g_0 = 2$ and $E_1 - E_0 \cong 1000$ cm^{-1}.

Alternatively the dilation contribution can be calculated according to Grüneisen [10] as:

$$C_d = \beta \Gamma C_v T$$

where Γ is the Grüneisen parameter. In the absence of knowledge of the compressibility of nickel selenides it is tentatively taken to be 2.5. The heat capacity of $Ni_{19}Se_{20}$ at constant pressure is seen to exceed the calculated values quite considerably at high temperatures and further contributions are thus of importance.

Theoretical treatments of anharmonic contributions to the heat capacity of solids [11–16] indicate that even at high temperatures the effects at constant volume are rather small and should therefore not be responsible for the discrepancy. Semiconducting properties have been reported [9] for the $Ni_{1-x}Se$-phase,

while metallic properties have been predicted.[17-21]. Conduction electrons might therefore be partly responsible for the enhanced heat capacity, but quantitative data are still lacking. Changes in the 3*d*-electron distribution seem, however, to be the major cause.

The ^3F ground state of the gaseous Ni^{2+} ion is split under the influence of an octahedral field into a lower triplet ($^3A_{2g}$) and two higher triplets ($^3T_{2g}$ and $^3T_{1g}$). If these states are of importance in the solid selenides, the changing population will contribute to the heat capacity of $Ni_{19}Se_{20}$. Considering the lower triplet only, transitions from a lower singly degenerate to a higher doubly degenerate state will give a maximum heat capacity contribution $C_m = 3.07$ J °K^{-1} per 0.487 mole nickel. This assumption will apparently explain most of the discrepancy between observed and calculated heat capacities up to about 700°K if the splitting is about 1000 cm^{-1}, see Fig. 4. In the localized electron approximation improved agreement is obtainable by assuming the upper doublet to be split, but the appropriate data are not available. Considerable doubt exists, however, with regard to the adequacy of the localized electron model.

At higher temperatures further levels are probably involved. An additional contribution to the heat capacity, due to compositional changes of the $Ni_{1-x}Se$-phase as the melting temperature is approached, is probably also of importance.

B. Ni_7Se_8. The heat-capacity behavior of Ni_7Se_8 is very similar to that of $Ni_{19}Se_{20}$ with the additional feature of a λ-type transition. An estimate of the entropy and enthalpy of the transition is obtained by subtracting the values for $Ni_{19}Se_{20}$ in the region 320 to 660°K, and leads to the values $\Delta S_{tr} = 0.96$ J °K^{-1} and $\Delta H_{tr} = 475$ J for 1/15 mole Ni_7Se_8.

This transition is obviously related to structural changes in the sample. X-Ray photographs were therefore taken at various temperatures and the results are shown in Table 4. The basic structure is hexagonal and of NiAs-

Table 4. Lattice sub-cell constants and volume for Ni_7Se_8. Units: °C, Å.

T	a	c	V
20	3.634	5.317	60.81
95	3.637	5.329	61.04
175	3.640	5.343	61.32
205	3.642	5.347	61.42
245	3.644	5.353	61.57
305	3.646	5.365	61.76
405	3.649	5.382	62.07
535	3.654	5.403	62.48

like type in the whole temperature range, but discontinuities are seen in the lattice constants around 500°K, especially for the a-axis, see Fig. 5. An orthorhombic structure with $A = a\sqrt{3}$, $B = 3a$, and $C = 3c$ has been observed [1] at room temperature. The superstructure reflections were so weak, however, that their presence could not be ascertained in the high-temperature camera used. Weissenberg photograph data indicate that the metal atom vacancies

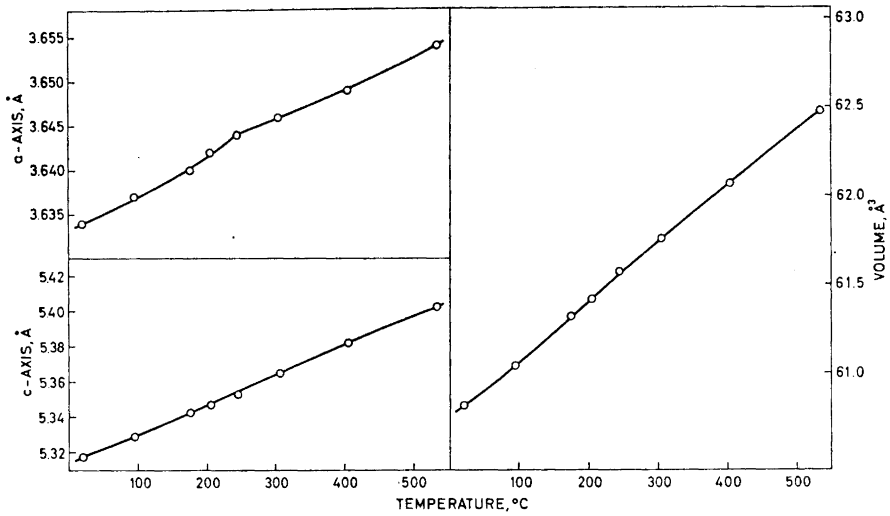

Fig. 5. Lattice constants and cell volume for the sub-cell of Ni_7Se_8.

are present in every other metal layer perpendicular to c and that they are ordered within these layers. The transition is therefore probably related to a vacancy order-disorder process, which is assumed to involve the partly vacant layers only. The resulting entropy increment of disorder is then

$\Delta S = -(R/2)(0.25 \ln 0.25 + 0.75 \ln 0.75) = 2.34$ J °K^{-1} per 0.875 mole of nickel atoms. The actually observed value $\Delta S_{tr} = 1.80$ J °K^{-1} per mole $Ni_{0.875}Se$, supports the assumption that the vacancies are largely ordered within every other nickel layer.

The smallest energy input in the 503°K transition region resulted in a temperature rise of 1.3°K. The heat capacity did not vary much with temperature in the peak region (*cf.* Series IX, runs 9 to 11) and the transition thus appears to be one of higher order. Conditions neccessary for higher-order transitions to occur are given in general terms by the Landau theory of phase transitions.[22] Application of the theory to compounds with NiAs-like structures by Haas [23] shows that in several cases the strict requirements are fulfilled. For the nickel selenides the exact structures are not yet known and no firm predictions can therefore be made.

C. Ni_4Se_5. For Ni_4Se_5 two λ-type transitions are observed. Estimates of the entropies and enthalpies of transition are obtained by subtracting the values derived from a smooth heat capacity curve over the region 440 to 780°K in case of the 589°K transition, and over the region 800 to 1020°K for the 995°K transition. For the 589°K transition $\Delta S_{tr} = 0.47$ J °K^{-1} and $\Delta H_{tr} = 265$ J for 1/9 mole Ni_4Se_5 while for the 995°K transition $\Delta S_{tr} = 0.13$ J °K^{-1} and $\Delta H_{tr} = 120$ J for the same amount of substance.

In order to explore the nature of the transitions, high temperature X-ray photographs were taken and the lattice constant data are shown in Table

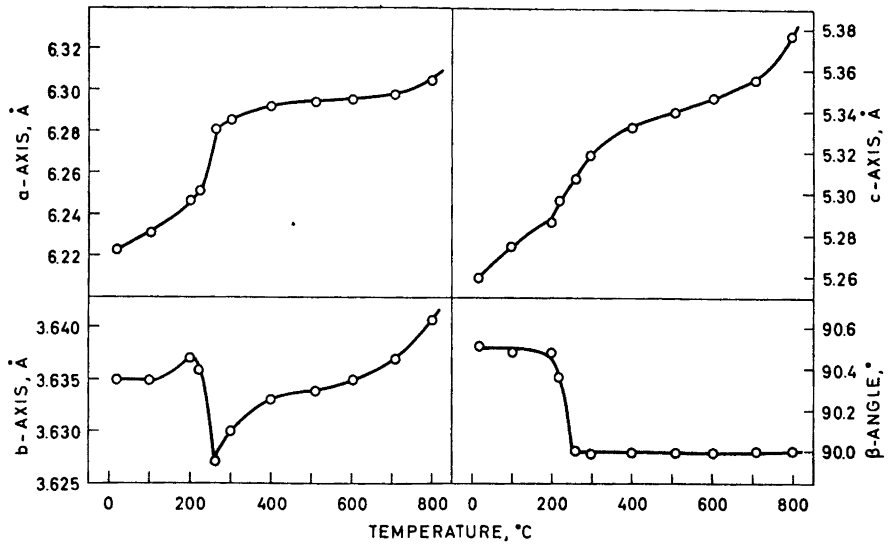

Fig. 6. Lattice constants for the sub-cell of Ni_4Se_5.

5 and Fig. 6. The structure of Ni_4Se_5 is monoclinic at room temperature with lattice constants in good agreement with earlier results.[1] The monoclinic angle stays approximately constant up to about 200°C and then changes rather abruptly to 90°. An almost discontinuous change in the length of the *b*-axis is also observed in the range 220 to 260°C. These phenomena take place at

Table 5. Lattice constants of Ni_4Se_5. Units: °C, Å, °.

T	$A(b\sqrt{3})$	b	C	β
20	6.224	3.635	2×5.260	90.52
100	6.231	3.635	2×5.275	90.49
200	6.248	3.637	2×5.286	90.48
220	6.252	3.636	5.298	90.36
260	(6.282)	3.627	5.308	90
300	(6.287)	3.620	5.320	90
400	(6.293)	3.633	5.333	90
510	(6.295)	3.634	5.341	90
605	(6.296)	3.635	5.347	90
710	(6.299)	3.637	5.366	90
800	(6.306)	3.641	5.377	90

temperatures below the observed maximum in heat capacity and indicate that important changes in symmetry and long range order occur in the first stages of the transition. The maximum in heat capacity is only reflected in the changing slope in the expansion curve for the *c*-axis around 300°C. No major

structural change occurs in the 995°K transition region, but a marked increase in expansivity apparently takes place, especially of the *c*-axis. It might, however, reflect the exsolution of selenium from the solid selenide.

New single-crystal data for Ni_4Se_5 indicate doubling also of the *b*-axis. This doubling is presumably related to the presence of additional nickel atoms in Ni_4Se_5 compared to an ideal compound Ni_3Se_4, in which every other nickel atom is missing in the partially vacant metal layers. Introduction of these atoms will lead to further correlations in the occupancy of sites which are responsible for the doubling of *b*-axis at low temperature. With increasing temperature this extra correlation disappears, and also the long-range correlations between vacant and occupied sites in the partially filled layers.

Judged from the heat capacity data, the transitions in Ni_4Se_5 are of higher order. The shape of the 589°K transition is somewhat broad, apparently because the heat capacity rises rather sharply in the beginning of the transition region, *i.e.* around 560°K. Thus, an intermediate structure might exist in the region 560 to 589°K, where the monoclinic deformation is still present but long-range correlation in the *c*-direction (doubling of the *c*-axis) no more exists.

The observed entropy increment of transition, $\Delta S_{tr} = 0.85$ J °K^{-1} per mole $Ni_{0.80}Se$, falls considerably short of that calculated for randomization of nickel atoms in every other layer perpendicular to the *c*-axis:

$\Delta S = -(R/2)(0.6 \ln 0.6 + 0.4 \ln 0.4) = 2.80$ J °K^{-1} per 0.80 mole of nickel atoms. The presence of a further transition with maximum at 995°K and an entropy increment $\Delta S_{tr} = 0.23$ J °K^{-1} per 0.80 mole of nickel atoms might indicate the disappearance of another long-range correlation, probably in the *ab*-plane (doubling of the *b*-axis?). It should also be noted that the entropy increments have been estimated rather conservatively, and that a considerably larger value, $\Delta S_{tr} = 1.6$ J °K^{-1} per mole $Ni_{0.80}Se$, is obtained if the data for $Ni_{19}Se_{20}$ are used to represent the non-transitional situation for $Ni_{0.80}Se$. Thus, the observed entropy increment of transition approximates that calculated by an admittedly crude model, and indicates that the zero-point configurational entropy in Ni_4Se_5 is of the order 1.5 J °K^{-1} for one mole $Ni_{0.80}Se$. The composition is, however, rather close to the ratio $Ni_{26}Se_{32}$ ($Ni_{0.813}Se$) at which complete structural order might possibly be reached.

Acknowledgements. The continued support by *Norges Almenvitenskapelige Forskningsråd* is gratefully acknowledged. The assistance of Nils Erik Askheim, Andreas Bugge, Nils Jørgen Kveseth, Bjørn Lyng Nielsen, Arvid Sveen and Jan Thorstensen in various phases of the time-consuming measurements and calculations is thankfully recognized. Rolf Møllerud kindly took some of the high temperature X-ray photographs. The selenium used was generously supplied by Bolidens Gruvaktiebolag.

REFERENCES

1. Grønvold, F. and Jacobsen, E. *Acta Chem Scand.* **10** (1956) 1440.
2. Grønvold, F. *Paper presented at the 2. Nordiske Strukturmøte*, Oslo 1955 see *Tidsskr. Kjemi Bergvesen Met.* **15** (1955) 49.
3. Hiller, J.-H. and Wegener, W. *Neues Jahrb. Mineral.* **94** (1960) 1147.
4. Grønvold, F. *Paper presented at the XVI International Congress of IUPAC*, Paris 1957.

5. Grønvold, F., Thurmann-Moe, T., Westrum, Jr., E. F. and Levitin, N. E. *Acta Chem. Scand.* **14** (1960) 634.
6. Grønvold, F. *Acta Chem. Scand.* **21** (1967) 1695.
7. Grønvold, F. *Acta Chem. Scand.* **22** (1968) 1219.
8. Nernst, W. and Lindemann, F. A. *Z. Elektrochem.* **19** (1911) 817.
9. Kuznetsov, V. G., Eliseev, A. A., Spak, Z. S., Palkina, K. K., Sokolova, M. A. and Dmitriev, A. V. *Voprosy Met. Fiz. Poluprov. Akad. Nauk SSSR* **1961** 159.
10. Grüneisen, E. *Ann. Phys.* **26** (1908) 393; **39** (1912) 257; See also *Handbuch der Physik* **10** (1926) 1.
11. Leibfried, G. and Ludwig, W. *Solid State Phys.* **12** (1961) 276.
12. Maradudin, A. A., Flinn, P. A. and Coldwell-Horsfall, R. A. *Ann. Phys. (N.Y.)* **15** (1961) 337, 360.
13. Maradudin, A. A., Montroll, E. W. and Weiss, H. G. *Solid State Phys. Suppl.* **3** (1963).
14. Wallace, D. C. *Phys. Rev.* **131** (1963) 2046.
15. Pathak, K. N. *Phys. Rev.* **139** (1965) A1569.
16. Barron, T. H. K. In *Lattice Dynamics*, Intern.Proc. Conf. Copenhagen, Denmark, Aug. 5.—9. 1963, Pergamon, New York 1965, p. 247.
17. Pearson, W. B. *Can. J. Phys.* **35** (1957) 8, 886.
18. Hulliger, F. *Helv. Phys. Acta* **32** (1959) 615.
19. Dudkin, L. D. *Vysokotemp. Metallorkeram. Materialy, Akad. Nauk Ukr. SSR* **1962** 87.
20. Dudkin, L. D. and Viidanich, V. I. *Voprosy Met. Fiz. Poluprov. Akad. Nauk SSSR* **1961** 113.
21. Hulliger, F. *J. Phys. Chem. Solids* **26** (1965) 639.
22. Landau, L. *Phys. Z. Sovjet.* **11** (1937) 26, 545; see also *Collected Papers of L. D. Landau*, Gordon and Breach, New York 1967, 193; L. D. Landau and E. M. Lifshitz, *Statistical Physics*, Pergamon, London 1958.
23. Haas, C. J. *Solid State Commun.* **4** (1966) 419.

Received August 1, 1969.